7-1-2004

Magnetization Processes in Melt-Spun Sm-Co-Based Alloys With the $TbCu_7$-Type Structure

A. Hsiaoa
Union College, Schenectady, NY, hsiaoa@union.edu

S. Aich
University of Nebraska - Lincoln, sham_04@hotmail.com

L. H. Lewis
Brookhaven National Laboratory, lhlewis@bnl.gov

Jeffrey E. Shield
University of Nebraska - Lincoln, jshield@unl.edu

Magnetization Processes in Melt-Spun Sm-Co-Based Alloys With the $TbCu_7$-Type Structure

A. Hsiao, S. Aich, L. H. Lewis, and J. E. Shield

***Abstract*—The initial magnetization processes in melt-spun Sm-Co alloys with remanent ratios above 0.7 have been studied. Alloys of $(Sm_{(1/(6+x)}Co_{(5+x)/(6+x)})_{94}Nb_3C_3$ ($x = 0.67$, 1.7, 2.3 and 3) alloys modified with Nb and C were melt spun at wheel speeds of 20 and 40 m/s, and the compositions span the range between the Sm_2Co_{17} and $SmCo_5$ stoichiometries. Structurally, all alloys formed in the $TbCu_7$-type structure, although a small amount of Sm_2Co_7 was observed in Sm-rich samples, and a small amount of fcc Co formed in Co-rich samples. From transmission electron microscopy analysis, grain sizes typically ranged from 100 to 500 nm, and the grains were randomly oriented. The as-spun ribbons had remanence ratios of 0.7 and coercivity values ranging from 3 to 18 kOe. The initial magnetization curves showed a steep linear response to the applied field for all samples, suggesting that nucleation-controlled processes dominate the magnetization process. In addition, the initial susceptibility decreased with increasing Sm content, reflecting the anisotropy differences between $SmCo_5$ and Sm_2Co_{17} compounds. The initial susceptibility also increased with increasing wheel speed, suggesting that the microstructure has important ramifications on the magnetization process as well.**

***Index Terms*—Anisotropy, permanent magnet, rapid solidification, remanence enhancement, SmCo alloys.**

I. Introduction

THE compounds found in Co-rich Sm-Co alloys are derivatives of the $SmCo_5$ structure. The equilibrium Sm_2Co_{17} compound, for example, substitutes a pair of Co atoms for a Sm atom. The substitution pattern can be systematic, as occurs in the Th_2Ni_{17}-type and Th_2Zn_{17}-type structures, or random, as occurs in the $TbCu_7$-type structure. Whereas the Th_2Ni_{17} and Th_2Zn_{17}-type structures are equilibrium structures, the $TbCu_7$-type structure is metastable. The formation of the $TbCu_7$-type $SmCo_7$ structure, has been accomplished by melt spinning, mechanical alloying, and dilute additions of Zr and Ti [1]–[4].

An important aspect of permanent magnet material design is the development of high remanence. High remanence is most often achieved through grain alignment or exploitation of exchange interactions in nanocrystalline grain structures. Generally, remanence enhancement arising from intergrain interactions requires the existence of grain sizes on the order of tens of nanometers [5]. In Sm-Co-based alloys, nanoscale structures have been recently achieved by rapid solidification combined with specific alloying additions [6], [7]. In this paper, we report on the magnetization processes in high remanence SmCo-based permanent magnets with a sub-micron, isotropic grain size. It will be demonstrated that the initial magnetization curves of these alloys show an increase in initial susceptibility with increasing Co content and slower wheel speeds, and a high remanence ratio is present for all compositions observed.

Manuscript received October 16, 2003. This work was performed in part under the auspices of the U.S. Department of Energy, Division of Materials Sciences, Office of Basic Energy Sciences, under Contract DE-AC02-98CH10886 and supported by the National Science Foundation under Grant DMR-0305354.

A. Hsiao is with the Department of Mechanical Engineering, Union College, Schenectady, NY 12308 USA (e-mail: hsiaoa@union.edu).

S. Aich and J. E. Shield are with the Department of Mechanical Engineering, University of Nebraska, Lincoln, NE 68588 USA (e-mail: sham_04@hotmail.com; jshield2@unl.edu).

L. H. Lewis is with the Materials Science Department, Brookhaven National Laboratory, Upton, NY USA (e-mail: lhlewis@bnl.gov).

Digital Object Identifier 10.1109/TMAG.2004.832118

II. Experimental Procedures

Alloys with the general composition $(Sm_{1/(6+x)}Co_{(5+x)/(6+x)})_{94}Nb_3C_3$ were arc-melted from high-purity elemental constituents with $x = 0.67$, 1.7, 2.3 and 3 corresponding to Sm/Co molar ratios of 15/85, 13/87, 12/88 and 11/89, respectively. These Sm/Co ratios span most of the compositional window between the Sm_2Co_{17} ($x = 3.5$) and $SmCo_5$ ($x = 0$) phases. To compensate for Sm loss due to its high vapor pressure, five weight percent excess Sm was added. Nb and C were added to promote the formation of the $TbCu_7$-type structure and refine the grain size [8]. The arc-melted ingots were then melt-spun at a tangential wheel speed of 20 m/s in an Ar atmosphere. Some compositions were also melt-spun at 40 m/s for comparison purposes. The resulting alloys were structurally characterized by x-ray diffraction (XRD) using CuK_α radiation, and transmission electron microscopy (TEM) using a JEOL 2010 microscope. Samples for TEM study were made by mounting the melt-spun ribbon on a Cu oval grid and ion milling to perforation using a Gatan Duomill or PIPS at 4.5 kV. Magnetization data were measured at 300 K with a Quantum Design SQUID MPMS magnetometer in the field range $-5T \leq H \leq 5T$. As the ribbons were measured with their long axes parallel to the field direction, no corrections for demagnetization effects were applied.

III. Results and Discussion

The phase constitution in the rapidly-solidified alloys as a function of composition was determined by XRD. For all alloys ($0.67 \leq x \leq 3$) the primary phase formed was $SmCo_7$ with the $TbCu_7$-type structure (Fig. 1). The combined effect of the rapid solidification and alloying with Nb suppressed the formation of the Sm_2Co_{17} equilibrium structure, which requires the ordering of transition metal dumbbells as discussed above. This result was similarly observed in rapid-solidification synthesis of analogous Sm-Fe alloys [8]. A higher resolution XRD scan taken at long counting times in the 2θ range 36°–40° confirmed the lack of long-range dumbbell ordering, as shown by the absence

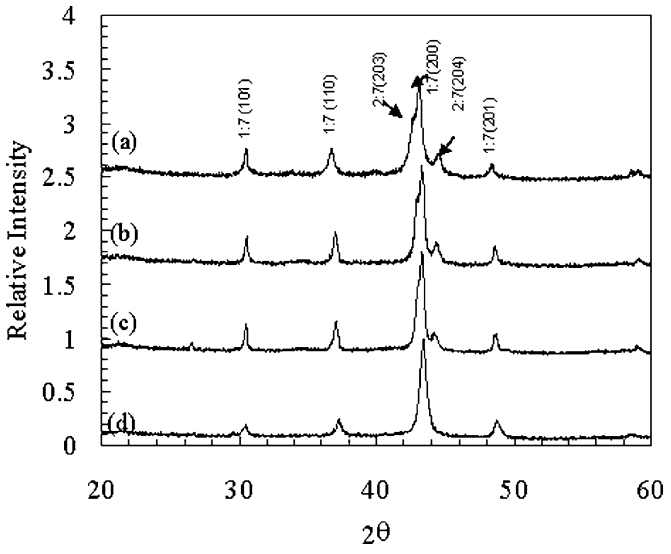

Fig. 1. X-ray diffraction pattern of rapidly solidified $(\mathrm{Sm}_{1/(6+x)}\mathrm{Co}_{(5+x)/(6+x)})_{94}\mathrm{Nb}_3\mathrm{C}_3$ alloys melt spun at 20 m/s corresponding to x= (a) 0.67, (b) 1.7, (c) 2.3, and (d) 3.

of the (024) superstructure peak predicted at $2\theta \sim 38.5°$. Only the fundamental peak [(110) indexed to the $\mathrm{TbCu_7}$ structure type, (300) indexed to the $\mathrm{Sm_2Co_{17}}$ structure] was observed for all of the alloys, even close to the stoichiometric 2:17 composition $(\mathrm{x} = 3)$. These results clearly indicate the presence of the $\mathrm{TbCu_7}$-type structure over a range of Sm/Co ratios. Thus the $\mathrm{TbCu_7}$ structure is found to exist over a solubility range, with differences in the structure ascribed to different concentrations of transition metal dumbbells arranged randomly in the structure. A change in the lattice parameters was observed as well [9], illustrated by the shift in the (110) peak to higher 2θ values with increasing x, also consistent with a variation in composition of the $\mathrm{TbCu_7}$-type structure.

In addition to the $\mathrm{TbCu_7}$-type structure formation, peaks indexing to the $\mathrm{Sm_2Co_7}$ structure can be observed in Fig. 1 for $\mathrm{x} < 3$. The relative amount of $\mathrm{Sm_2Co_7}$ decreased with increasing x, so that at $\mathrm{x} = 3$ the material was pure $\mathrm{SmCo_7}$, within the detection limits of XRD. The presence of the $\mathrm{Sm_2Co_7}$ phase was unexpected considering the equilibrium phase diagram [10], which indicates the existence of a eutectic between the 2:17 and 1:5 compounds. Thus, solidification within this composition range should only result in the formation of $\mathrm{Sm_2Co_{17}}$ and $\mathrm{SmCo_5}$. The observation of $\mathrm{Sm_2Co_7}$, decreasing in quantity with increasing Co concentration, suggests a peritectic solidification process. The nonequilibrium processing and the influence of Nb alter the solidification processes, exposing underlying metastable behavior [11]. Consideration of XRD patterns obtained from the wheel-side and the free-side of the melt-spun ribbons show that there is no crystallographic texture found in the ribbons.

The grain size varied little with composition and was on the order of 200–500 nm for alloys melt spun at 20 m/s (Fig. 2). Electron diffraction corroborated XRD results in revealing crystallographically isotropic grain structures. The grains were also relatively equiaxed. It is also important to note that in general no cellular structure characteristic of sintered Sm-Co alloys was observed.

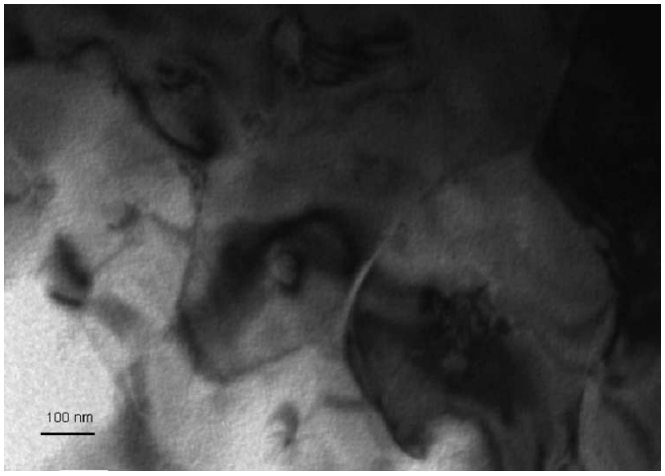

Fig. 2. Transmission electron micrograph of $(\mathrm{Sm}_{1/(6+x)}\mathrm{Co}_{(5+x)/(6+x)})_{94}\mathrm{Nb}_3\mathrm{C}_3$ with $\mathrm{x} = 1.7$ (Sm/Co ratio of 13/87) melt spun at 20 m/s showing typical microstructure.

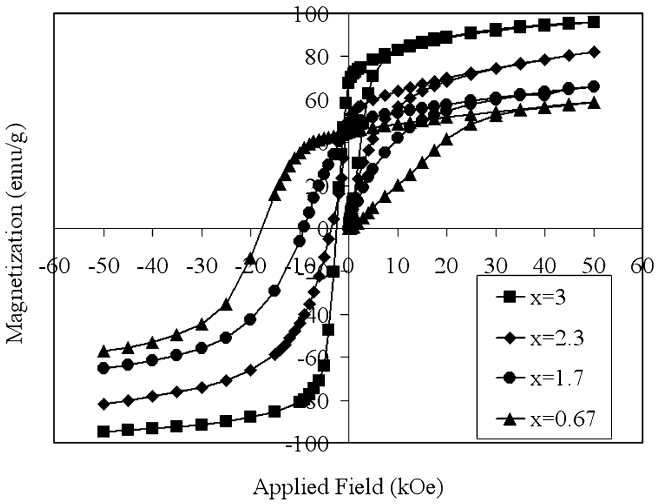

Fig. 3. Magnetization as a function of applied field for $\mathrm{TbCu_7}$-type alloy ribbons with different values of x melt spun at 20 m/s.

Magnetic data from the samples melt-spun at 20 m/sec are shown in Fig. 3. The initial magnetization curves show a steep initial susceptibility that increases with increasing Co content. This steep initial response is indicative of nucleation-controlled magnetization processes. However, the initial susceptibility is somewhat lower than dM/dH at the coercivity ${}_{\mathrm{i}}\mathrm{H_c}$, suggesting a combined magnetization processes but dominated by nucleation. Sintered $\mathrm{Sm_2Co_{17}}$-based magnets tend to display mixed nucleation and pinning modes as well, but are dominated by pinning [12], and Sm-Co-Cu-Ti alloys produced by mechanical milling also showed a low initial susceptibility characteristic of pinning-dominated mechanisms [13]. The nucleation-controlled behavior may be the result of the similarities in crystal structures between the $\mathrm{TbCu_7}$-type and $\mathrm{SmCo_5}$ structures, and the lack of strong pinning centers characteristic of cellular 2:17 magnets.

The increasing initial susceptibilility with increasing Co content in the present alloys is believed to be a reflection of decreasing magnetocrystalline anisotropy of the $\mathrm{SmCo_7}$ compound with increasing Co content [9]. The demagnetization

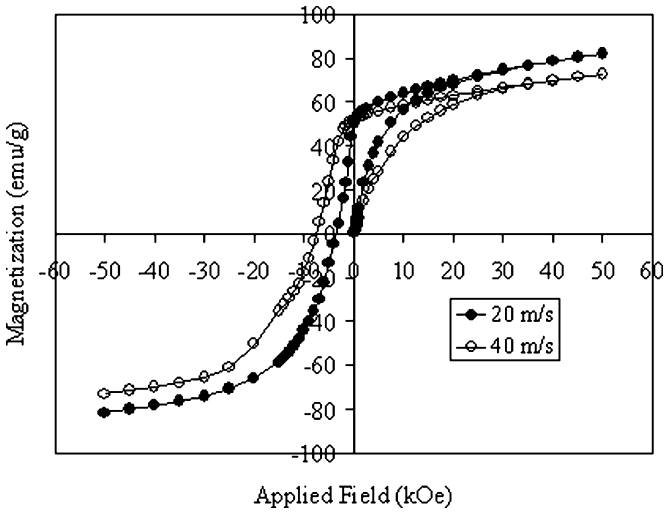

Fig. 4. Initial susceptibility as a function of wheel speed for $x = 2.3$ melt-spun alloy.

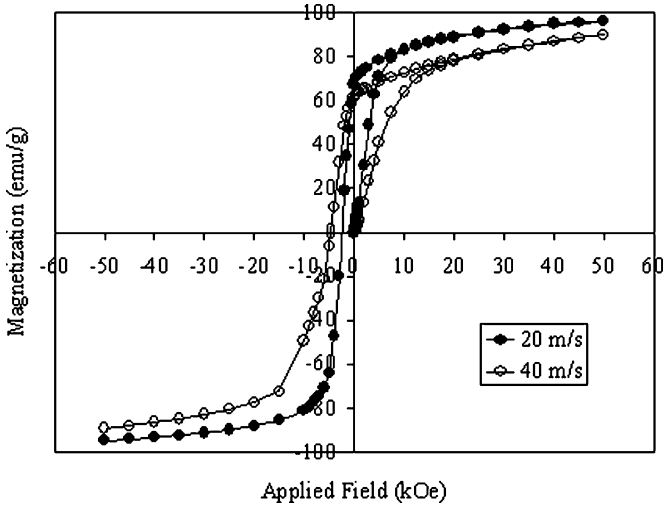

Fig. 5. Initial susceptibility as a function of wheel speed for $x = 3$ melt-spun alloy.

behavior from the saturated state and the coercivity trend, as shown in Fig. 3, also reflects a decrease in magnetocrystalline anisotropy with increasing Co content. Significant coercive forces approaching 20 kOe were observed for low x. The room-temperature energy products of these alloys range from 4 to 6 MGOe.

A smooth second-quadrant demagnetization behavior is observed in these alloys, characteristic of single magnetic phase behavior. What is remarkable about Fig. 3 is the extremely high remanence ratio $(M_r/M_s \approx 0.7)$ observed for all compositions. This value is significant considering that the grain size of these samples is on the order of a few hundred nanometers, well above the limit normally associated with intergranular isotropic exchange-coupled systems [5]. The remanence enhancement does not appear to arise from crystallographic texture either, as no preferred orientation of grains was observed. The origin of the remanence enhancement is not clear at this time.

Alloys with $x = 2.3$ and 3 were also melt spun at 40 m/s. The phase formation was similar to that of the alloys melt spun at 20 m/s. The initial magnetization curves were also similar, with a steep initial increase in magnetization with low increasing fields (Figs. 4 and 5). Ribbons obtained at the higher wheel speed, which produces a finer grain size, display a lower initial susceptibility than their lower wheel-speed counterparts. A notable increase in the coercivity of the ribbons is found at the higher wheel speeds. The lower initial susceptibility and higher coercivity observed in the samples melt spun at higher wheel speeds suggests that all other factors constant, the microstructure, notably the grain size, still significantly influences the magnetization processes in this intermediate grain size regime.

IV. Conclusions

The room-temperature magnetization behavior has been studied for a series of melt-spun Sm-Co alloys with the $TbCu_7$-type structure and correlated with composition and microstructure. All samples showed remarkably high remanent ratios of 0.7. In all cases, initial magnetization curves displayed sharp increases with increasing low fields, characteristic of nucleation-controlled magnetization processes. The initial susceptibility decreased with increasing Sm content throughout the $TbCu_7$-type solid solution region, reflecting the change in the magnetocrystalline anisotropy with composition. Higher wheel speeds generated finer microstructures and resulted in lower initial susceptibilities and higher coercivities than their counterparts melt spun at lower wheel speeds.

References

[1] H. Saito, M. Takahashi, T. Wakiyama, G. Kido, and H. Nakagawa, "Magnetocrystalline anisotropy for $Sm_2(Sm, Mn)_{17}$ compound with $TbCu_7$-type disordered structure," *J. Magn. Magn. Mater.*, vol. 82, pp. 322–326, 1989.

[2] M. Q. Huang, W. E. Wallace, M. E. McHenry, Q. Chen, and B. M. Ma, "Structure and magnetic properties of $SmCo_{7-x}Zr_x$ alloys $(x = 0 - 0.8)$," *J. Appl. Phys.*, vol. 83, pp. 6718–6720, 1998.

[3] M. Q. Huang, M. Drennan, W. E. Wallace, M. E. McHenry, Q. Chen, and B. M. Ma, "Structure and magnetic properties of $RCo_{7-x}Zr_x$ ($R = Pr$ or Er, $x = 0 - 0.8$)," *J. Appl. Phys.*, vol. 85, pp. 5663–5665, 1999.

[4] J. Zhou, I. A. Al-Omari, J. P. Liu, and D. J. Sellmyer, "Structure and magnetic properties of $SmCo_{7-x}Ti_x$ with $TbCu_7$-type structure," *J. Appl. Phys.*, vol. 87, pp. 5299–5301, 2000.

[5] H. A. Davies, "Nanocrystalline exchange-enhanced hard magnetic alloys," *J. Magn. Magn. Mater.*, vol. 157/158, pp. 11–14, 1996.

[6] W. Manrakhan, L. Withanawasam, X. Meng-Burany, W. Gong, and G. C. Hadjipanayis, "Melt-spun $Sm(CoFeCuZr)_zM_x$ ($M = B$ or C) nanocomposite magnets," *IEEE Trans. Magn.*, vol. 31, pp. 3898–3900, 1997.

[7] S. S. Makridis, G. Litsardakis, I. Panagiotopoulos, D. Niarchos, and G. C. Hadjipanayis, "Effects of boron substitution on the structural and magnetic properties of melt-spun $Sm(Co, Fe, Zr)_{7.5}$ and $Sm(Co, Fe, Zr, Cu)_{7.5}$ magnets," *J. Appl. Phys.*, vol. 91, pp. 7899–7901, 2002.

[8] B. E. Meacham and J. E. Shield, "The combined effect of metal carbide additions on the microstructure and structure of Sm_2Fe_{17}," *J. Mater. Res.*, vol. 18, pp. 279–283, 2003.

[9] S. Aich and J. E. Shield, "Phase formation and magnetic properties of $SmCo_{5+x}$ alloys with the $TbCu_7$-type structure," *J. Magn. Magn. Mater.*, to be published.

[10] H. Baker *et al.*, Ed., *Alloy Phase Diagrams*. Metals Park, OH: ASM International, 1992.

[11] J. E. Shield, unpublished, .

[12] X. Chen, J. F. Liu, C. Ni, G. Hadjipanayis, and A. Kim, "Magnetic and structural properties of commercial $Sm_2(Co, Fe, Cu, Zr)_{17}$-based magnets," *J. Appl. Phys.*, vol. 83, pp. 7139–7141, 1998.

[13] J. Zhou, R. Skomski, C. Chen, G. C. Hadjipanayis, and D. J. Sellmyer, "Sm-Co-Cu-Ti high-temperature permanent magnets," *Appl. Phys. Lett.*, vol. 77, pp. 1514–1516, 2000.